Chapter 8

A Test Facility to Investigate Sheath Effects during Ion Cyclotron Resonance Heating

Kristel Crombe, Rodolphe D' Inca, Eric Faudot, Helmut Faugel, Ana Kostic, Mariia Usoltceva, Jean-Marie Noterdaeme, Anton Nikiforov, Helmut Fuenfgelder, Stephane Heuraux, Jonathan Jacquot, Fabrice Louche, Roman Ochoukov, Ilya Shesterikov and Dirk Van Eester

Additional information is available at the end of the chapter

http://dx.doi.org/10.5772/intechopen.76730

Abstract

Nuclear fusion is a promising candidate to supply energy for future generations. At the high temperatures needed for the nuclei to fuse, ions and electrons are no longer bound into atoms. Magnetic fields confine the resulting plasma. One of the heating methods is the ion cyclotron resonant absorption of waves emitted by an external Ion Cyclotron Radio Frequency (ICRF) antenna. The efficiency of ICRF heating is strongly affected by rectified RF electric fields at antenna and other in-vessel components (so-called 'sheath effects'). The chapter presents an overview of ICRF principles. Attention is given to characterising the detrimental sheath effects through experiments on a dedicated test facility (IShTAR: Ion cyclotron Sheath Test ARrangement). IShTAR has a linear magnetic configuration and is equipped with an independent helicon plasma source. The configuration and capabilities of the test-bed and its diagnostics are described, as well as an analysis of the plasmas.

Keywords: plasma, helicon, radio frequency, sheaths, diagnostics

1. Introduction

IShTAR (Ion cyclotron Sheath Test ARrangement) is a linear magnetised plasma test facility for RF sheaths studies at the Max-Planck-Institut fuer Plasmaphysik in Garching (IPP-Garching), Germany. The test facility consists of a cylindrical vacuum vessel with a diameter of 1 m and length of 1.1 m. The plasma is created by an external cylindrical plasma source equipped with a helical antenna that has been designed to excite the m = 1 helicon mode. In contrast to a tokamak, a test stand provides more liberty to impose the parameters and gives better access for the instrumentation and antennas. The project also supports the development of diagnostic methods for characterising RF sheaths and validating and improving the theoretical predictions.

The present specific application is to analyse the formation of RF sheaths when waves in the Ion Cyclotron Range of Frequencies (ICRF) are injected in the plasma. In tokamaks, they have been successfully used to heat the plasmas to the nuclear fusion relevant temperatures of around 10 keV [1], but experimental and theoretical studies have shown that several spurious edge plasma interactions can prevent an optimal coupling if effects are forgotten or misunderstood. Particularly, the RF sheaths are created on the antenna surface and on limiters by the large $E_\parallel$ (parallel to the background magnetic field) component of the Slow Wave (SW) from the antenna [2, 3]. Under this field, the electrons with a lighter mass are more prone to be expelled from the plasma than the heavier ions: this creates a net positive DC voltage, called rectified sheath potential which conserves the charge ambipolarity. The additional DC potential raises the energy of the ions knocking the wall, the sputtering increases, hot spots are generated and more impurities are released into the plasma. At the same time the RF power losses become more pronounced [4–6]. Even though extensive studies have been carried out in the last years and the understanding has improved [7], a definitive solution is still pending because a systematic investigation cannot be done efficiently in the main fusion experiments. There are several reasons: the experimental time allocated to the topic is limited; the access, location and operations of diagnostics dedicated to RF sheath properties is constrained by other instruments, by the machine operation parameters and by the plasma itself. The application of corrective measures or the test of new antenna designs is constrained by the limited opening time of the tokamak and by the interfaces with the access port and the surrounding wall. Therefore, a dedicated test-bed offering more working time has been developed and assembled, in which it is possible to launch the waves using different antenna designs. More time can be devoted to the analysis of RF sheaths effects. New diagnostics to measure plasma parameters and electromagnetic fields in front of the ICRF antenna can be tested and the results can be compared with existing theoretical models of the sheath rectification effect. Different types of solutions emerging from modelling can be tested. In addition, other interesting phenomena related to antenna-plasma coupling can be analysed: sheath-plasma waves and resonances, effect of fast ions, plasma breakdown and wall conditioning by the ICRF antenna. In the first part, the constraints, which guided the initial choice and the operating parameters, are discussed. It is followed by a description of the resulting design and architecture of the facility. In the last part, first operations and measurements are illustrated, to conclude with the next steps and extension plans for the diagnostic instrumentation.

http://dx.doi.org/10.5772/intechopen.76730

2. Requirements and constraints

In this section the requirements, which were used to guide the design of the test-bed, are discussed. IShTAR is designed with the main purpose of investigating the RF sheath effects [8]. It is thus important to relate its functional parameters to the characteristics of a tokamak in the vicinity of the ICRF antenna.

2.1. Functional requirements

The main requirement for a test-bed dedicated to the analysis of ICRF antenna/plasma coupling, independent of the type of topic studied, is the geometry of the configuration, which has to be as similar as possible to the tokamak edge. This requires a vacuum vessel with a curved wall, a support to mount the ICRF antenna and a port for the RF feeding lines. A magnetised plasma is present and located only few centimetres away from the antenna (typically 15–20 cm). To simplify the configuration the magnetic lines are straight. Two main design factors have an important impact for the sheath studies: the plasma parameters and the antenna frequency. The former constrains the design of the plasma source and the second the choice of generator and matching system for the ICRF antenna. These factors determine the type of waves that are coupled and whether they are able to propagate, or not, in the plasma. The main parameters for the plasma are: the gas type, magnetic field, density and temperature. In a homogeneous, magnetised plasma, the wave equation reads:

$$\bar{k} \times (\bar{k} \times \bar{E}) + k_0^2 \bar{K} \cdot \bar{E} = 0, \tag{1}$$

where $\bar{k}$ is the wave vector, $\bar{E}$ the electric field associated with the wave, ω the angular frequency of the wave in vacuum, $k_0 = \omega / c$ the vacuum wavelength with c the speed of light and $\bar{K}$ is the plasma dielectric tensor. A detailed study of the wave propagation in IShTAR can be found in [9]. The main purpose of the test-bed is to provide conditions where the dispersion relation of the fast wave (used for heating) and of the slow wave (which produces the RF sheath) are similar to the tokamak case. Cold plasma calculations have been done for the reference case of a tokamak. It is plotted in **Figure 1b**. The operational parameters (magnetic field, ICRF frequency) of the test-bed have been varied to get similar wave behaviour as for the tokamak case, where slow and fast waves are well distinguished (**Figure 1a**).

2.2. Operational requirements

The main operational constraint for the operation and maintenance of the machine is the flexibility and accessibility: this is what makes the difference between the tokamak and the test-bed. We will see in the design section that the requirements lead to a machine with an important level of complexity. It is necessary that it does not impede an easy access to the machine or impose long time of preparation before the experiments. Therefore we have the following requirements on the operations and on the maintenance:

1. Start-up sequence duration shorter than an hour: from initial sleep phase at atmospheric pressure to first plasma in vacuum with full instrumentation. This has an impact on the

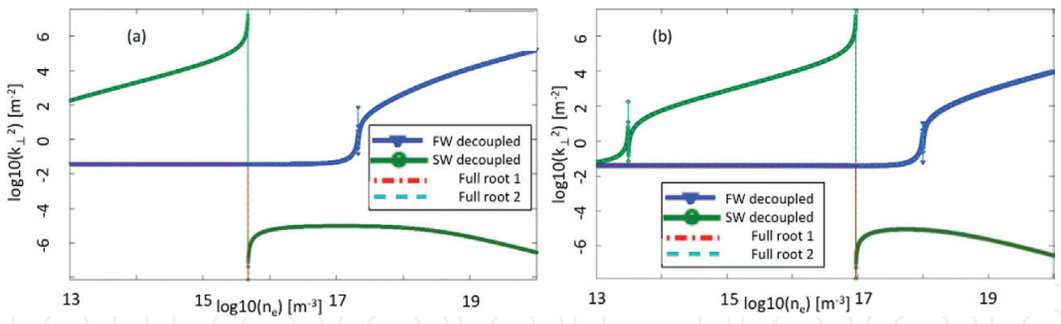

Figure 1. $k_{\perp}^{2}$ values for full and decoupled solutions as a function of the plasma density. (a) The reference case of *ISh*TAR for typical operating conditions: f = 5 MHz, Bt = 0.1T, Te = 10 eV and plasma composition: 100% Ar. (b) A tokamak scenario with: f = 50 MHz, Bt = 2T, Te = 10 eV, plasma composition: 95% D, 5% H. The notation "log10" denotes sign (F) log10 (|F|) when |F| > 1 and 0 when |F| < 1. It is introduced to enable capturing the very different length scales of the modes the cold plasma supports while allowing to identify regions of wave propagation and evanescence by a mere glance of the sign of log10 ($k_{\perp}^{2}$). In the low density region, both roots approach the vacuum limit, $k_{\perp}^{2} = k_{0}^{2} - k_{//}^{2}$, as expected, while at higher densities representative for the core one root is propagative (fast wave FW) and the other is deeply evanescent (slow wave SW).

speed of the vacuum pumps and on the control system, which has to be fully automatized. The purpose is to be able to do short iterations between experiments and analysis.

2. Short vessel opening and closing durations: it should be possible to open the vessel, install new components (like an antenna) and close the vessel in a couple of days; here again, it helps to have short iteration times between the installation of new solutions, their test and the analysis of their impact.

3. The "plug and play" instrumentation platform: the test-bed enables the analysis of many different phenomena requiring different types of diagnostics, either of in-house origin or provided by external teams. The control and acquisition system has to be universal enough to reduce the time between the installation of the instrument and the exploitation of its data in the centralised discharge database.

2.3. Cost control

The last constraint comes from the costs. To keep the costs under control, not all components were designed from scratch. Several have been refurbished from previous experiments. Among the most important ones is the main vacuum vessel with its 8 kA magnetic coils, the smaller coils and the ICRF generator, which comes from the WEGA stellarator. The downside is that their range of operation or geometry can limit the operational parameter space. This overview of the requirements clarifies the guidelines for the design of the facility.

3. Design and setup

The main design choice concerns the creation of the plasma in front of the ICRF antenna: either the ICRF itself can breakdown the gas or an external source can be used. Both solutions have been retained for the final design.

http://dx.doi.org/10.5772/intechopen.76730

The ICRF antenna itself can create plasma. The electrons are heated by the parallel component (parallel to the B-field) of the RF electric field. The advantage would be that no other means than the ICRF components are needed to create the plasma. But there are three disadvantages: first, the plan is to test different types of antenna and it will be difficult to reproduce the same plasma with different geometries. Second, the physics of plasma breakdown with ICRF antennas is still not completely understood. And third, the parallel electric field used for the breakdown is the same that creates the RF sheath: it may be difficult to disentangle both phenomena [10].

An external plasma source solves this problem by separating the plasma creation from the plasma heating. The concept of a helicon discharge [11–13] has been retained: it is compatible with the magnetic field and it creates high densities in large volumes. However, the solution has a price: the physics of helicon sources is still an area of investigation; it requires large amount of power to ionise the plasma volume required; it adds a new wave inside the plasma, which can interact—depending on the frequency—with the ICRF waves. Therefore, a backup solution exists with the use of a more classical inductive coil.

The test-bed has therefore two large components: the main vessel where the ICRF antenna is installed and connected to the power transmission lines; and the plasma source, connected with an open port to the main vessel, which generates the plasma that will flow in front of the antenna. These systems are connected to power generators, gas feeding lines, DC current modules and real-time controllers to monitor the operations and the safety of the test-bed. An overview of the facility is depicted in **Figure 2**; the characteristics of different components are explained in the next subsections.

3.1. Vacuum vessel

The vacuum vessel has a cylindrical geometry. The length is 1126 mm and the diameter (D) is 1000 mm. There are five ports in the wall: two horizontal ports (D = 225 mm) on one side which

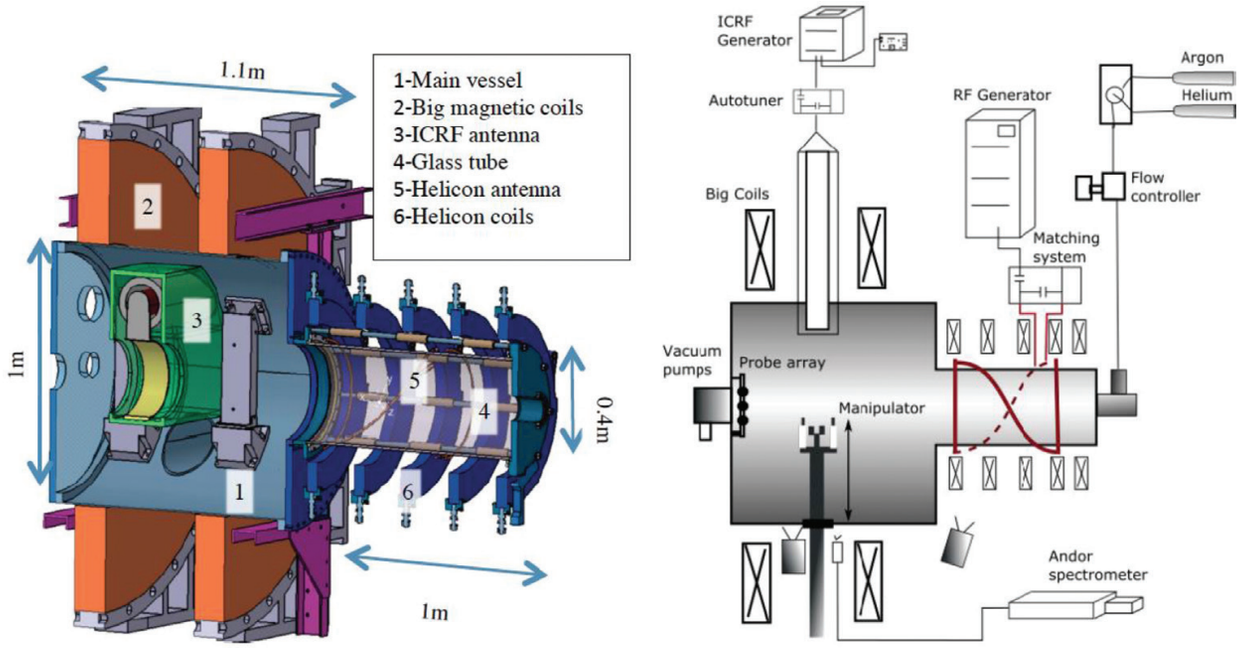

Figure 2. Overview of the different components of IShTAR.

can be used to connect the RF transmission line for the ICRF antenna and pressure gauges and valves, and, on the opposite side, one large horizontal port (D = 225 mm) and two smaller ports (D = 100 mm) angled at approximately 30 degrees with respect to the horizontal line. All ports have the same axial position, at 391 mm from the back end of the cylinder. On both ends of the vessel, there are two flanges with the following glass windows: at the back end, three large windows (D = 160 mm) and two small panels (D = 105 mm) at one end; at the front end, two large ports (D = 400 mm) and two small windows (D = 105 mm). The plasma source is connected to one of the front large ports. In the first months of operation it was not centred with respect to the axis of the main vessel, which resulted in instable operating conditions. Therefore later on the connecting flange was changed and now the helical source and main vessel are aligned. The vacuum system is connected to the back flange and consists of a pre-vacuum pump to reach a pressure of 10^{-2} mbar and a turbo molecular pump to create a high vacuum at 10^{-6} mbar. These pumps have a large flow rate making; the minimal pressure can be reached in 30 min time.

3.2. Large magnetic field coils

The main vessel is equipped with two magnetic coils in a Helmholtz configuration. The distance between the coils is about 815 mm. Some of the characteristics are given in **Table 1**. The outer/inner diameter is 2200/1200 mm and the thickness varies between 120 and 180 mm. The coils are connected to the central high current supply of the institute, which uses two modules connected either in parallel or in series using regular electrical voltage at 10.5 kV at 50 Hz. The magnetic (B) field in the centre of the vacuum vessel is expected to be 0.1 T for a current of 2.4 kA in the main coils. Higher currents and fields are possible. The current generator can sustain 4 kA for 10s and 12kA for 1 s, corresponding with B-fields up to 0.275 and 0.4 T respectively.

3.3. External plasma source

The plasma source is based on the concept of ionisation by helicon waves, which offer the possibility for large volumes to reach high densities (10^{18} m^{-3} and above) with uniform radial profiles

	Large coils	**Small coils**
Inductance L	0.4 mH	1.74 mH
Resistance R	0.86 mΩ	1.54 mΩ
Maximal current	47 kA	10 kA
Maximal voltage	3 kV	12 V
Time constant τ	0.5 s	n.a.
Pulsed current	4 kA	1 kA
Nominal current	1.5 kA	n.a.
Nominal voltage	600 or 340 kV	n.a.
Pulse length	10 s	10 s
Duty cycle	5.6%	n.a.

Table 1. Characteristics of the large and small coils.

http://dx.doi.org/10.5772/intechopen.76730

[10–12]. The price for this objective is the high level of injected power (several kW), which can lead to dramatic damages if the flow of the power in the source is not controlled. To reduce the risks the operations will be carried out first in inductive mode and, by progressively increasing the available power on the generator, we will try to reach the mode transition to the helicon mode. The source includes a glass tube as vacuum vessel, four magnetic coils (the helicon wave is a magnetised wave), a helical antenna with its own power supply and a gas injector.

The most risk prone component is the glass tube, which faces the following dangers:

i. Arcing: the risk is to hit and break the glass tube. If only inductive discharges would be generated, it would be possible to install a shield to protect the tube (with the advantage to remove spurious capacitive effects in the plasma); however, with helicon plasmas, the electrostatic component is necessary as well. Therefore, before increasing the power, we need to investigate the distribution of RF fields in the plasma source and check that we are able to have a good absorption in the plasma (decreasing the voltage on the antenna). Even with that, an arc detection system may be necessary to prevent in a very short time the development of an arc.

ii. Heat fluxes: the glass tube is made of borosilicate glass Duran with a safe maximum temperature of 150 and 500°C if it is submitted to homogeneous fluxes on its surface. Given its specific heat capacity Cp = 750 J/(kg °C), a mass of 17 kg and a discharge duration of 8 s, it can sustain a flux of 250 W at 150°C.

iii. Sputtering: this is the unknown and will require a better analysis. Previous experiments show an increase of the sputtering during helicon discharges, but variable from machine to machine.

The characteristics of the helicon magnetic coils are displayed in **Table 1**. These small coils are fed with a power supply DC10, with current between 0 and 1 kA, and voltage of 10 V. The maximum field inside the source is 0.1 T. In standard operation, this field is superimposed on the field generated by the large coils. The structure with the helicon in its central position is presented in **Figure 3** for a current of 1kA in the large coils and 0.45 kA in the small coils. The resulting B-field in the centre of the vessel is around 40 mT. By adapting the ratio in the field in small and large coils the plasma performance can be influenced. The optimisation of the performance is the subject of on-going research.

The test-bed flexibility makes it possible to test different types of antennas. The presently mounted antenna is a Shoji III half turn [14]. In other experiments, it proved to have a better coupling, especially with the mode m = 1. It has a length $L_a = 1$ m and diameter $d_a = 0.6$ m. The dispersion relation of the helicon wave sets a relation between the minimal density for which the wave can propagate and the magnetic field [14]:

$$kk_z = \frac{e\,\mu_0\,n_e\,\omega}{B_0}, \tag{2}$$

k is the total wave number, k_z is the longitudinal wave number, e is the electron charge, μ_0 is the vacuum permeability, n_e is the electron density, ω is the pulsation of the generator and B_0 is the static magnetic field.

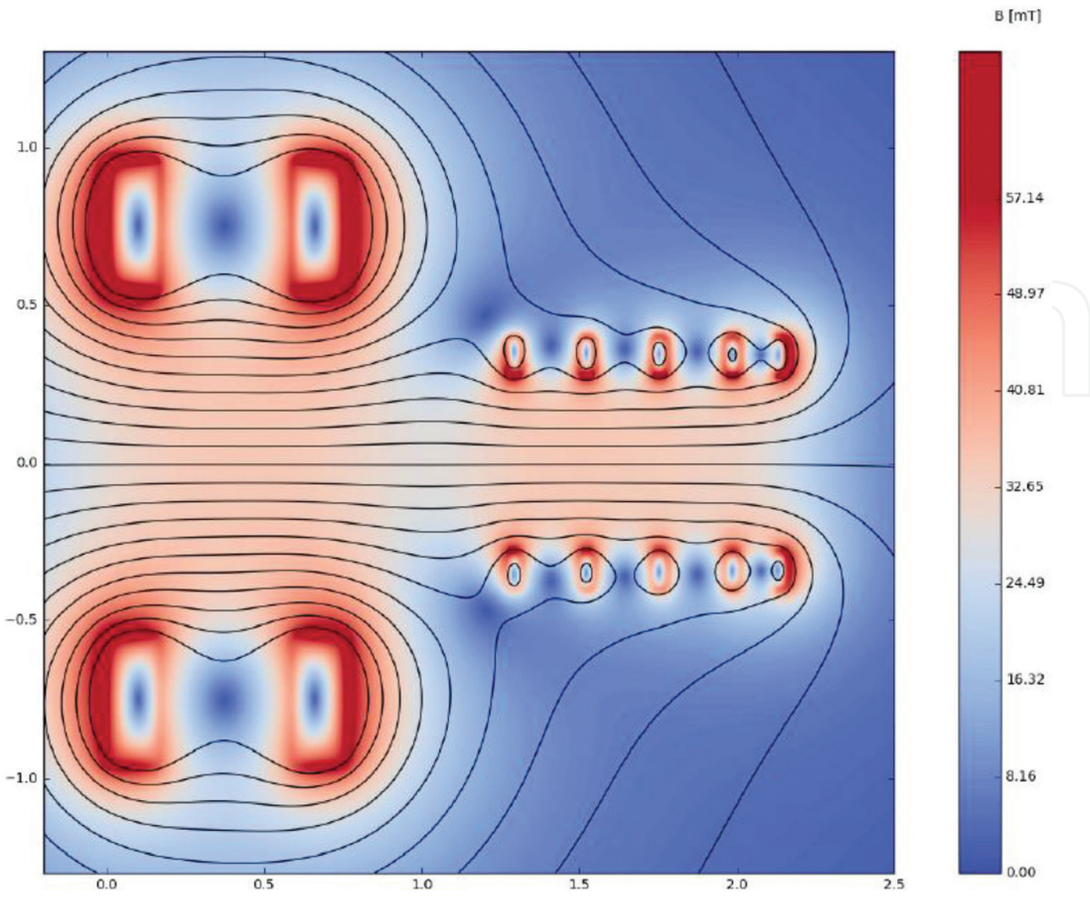

Figure 3. Example of a typical magnetic field topology for IShTAR (in mT). It is generated with currents of 1 kA in the large coils and 0.45 kA in the small coils.

k_z is determined by the geometry of the antenna:

$$k_z = (2\kappa + 1)\frac{\pi}{L_A}, \tag{3}$$

where κ is the longitudinal mode number and L_A is the length of the antenna.

The radial wavenumber k_r is determined from the calculation of the electrical field in a cylindrical geometry (in a simple case with constant density). This relation is represented for the mode m = 0 in **Figure 4**. For a maximum field B = 0.1 T in the plasma source, a density $n_i \approx 7\ 10^{16}$ m^{-3} is necessary for the helicon wave to propagate. The low frequency has been chosen based on simulations with the electromagnetic code MicroWave Studio (MWS) [15] (with a simple dielectric) to minimise the electric fields and the risk of arcing.

The plasma source is equipped with a gas valve at the back of the tube with a flow rate range of 5–5000 sccm. Three gases can routinely be used: argon, helium and hydrogen with three different feeding lines.

3.4. Control system

The control system automates the experiments, enables a fast start and remote operations, and it is possible to monitor the status of the different parameters (pressure, temperature,

http://dx.doi.org/10.5772/intechopen.76730

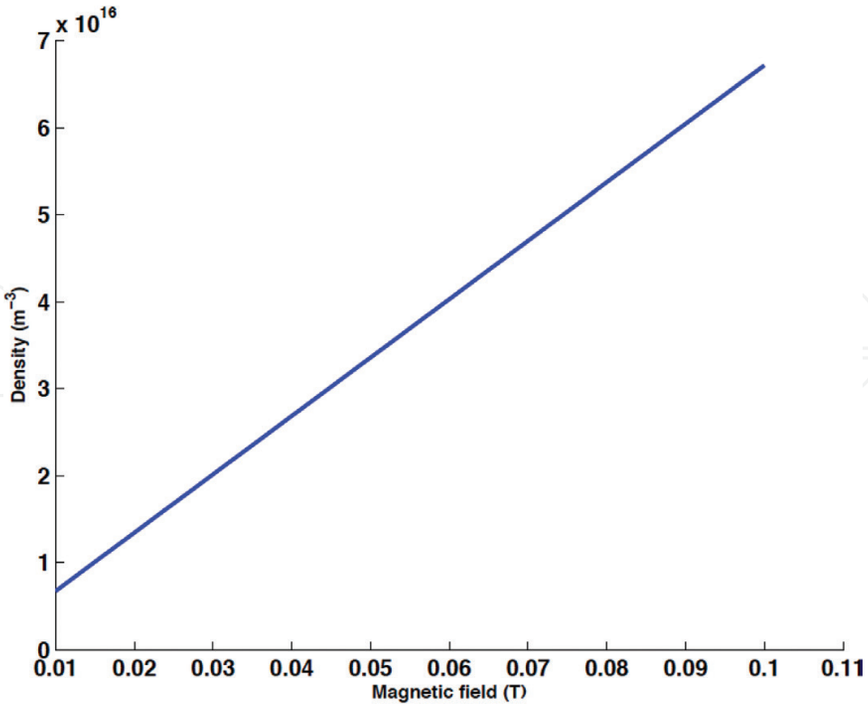

Figure 4. Minimum density required for the helicon mode $m = 0$ to propagate as a function of the magnetic field for the chosen antenna parameters $f = 11.7$ MHz, length = 1 m, radius $r_a = 0.3$ m.

current) of the test-bed. The control is based on a Simatic system for the hardware and WinCC applications for the software with a time step of 10 ms; it controls the automatic opening and closing of the valves and pumps during the vacuum build-up and re-pressurisation. It also enables the operator to define ramps in the coil current. It ensures the safety of operation by keeping the access doors locked below a predefined vacuum level in the vessel, checking the flow of coolant in the different components.

3.5. ICRF system

A mock-up of an operational ICRF antenna can be installed on the wall of the vessel and connected on one of the side ports to the transmission line, which is equipped with a ceramic vacuum window. Two RF power sources are presently available for the ICRF system:

i. One ASDEX Upgrade RF generator (30–120 MHz) with a power up to 2 MW at 30–80 MHz and 1 MW at 80–120 MHz.

ii. A broadband amplifier with an output power of 1 kW in the frequency range 100 kHz to 100 MHz.

The matching of the ASDEX Upgrade generator is insured by a system of two stub tuners. The broadband amplifier requires the installation of an additional capacitor-base matching network more suited to low levels of power.

3.6. ICRF antenna

An ICRF antenna was designed at the Laboratory for Plasma Physics in Brussels, Belgium (LPP-ERM/KMS) and installed in IShTAR. The MicroWave Studio (MWS) [15] model of the

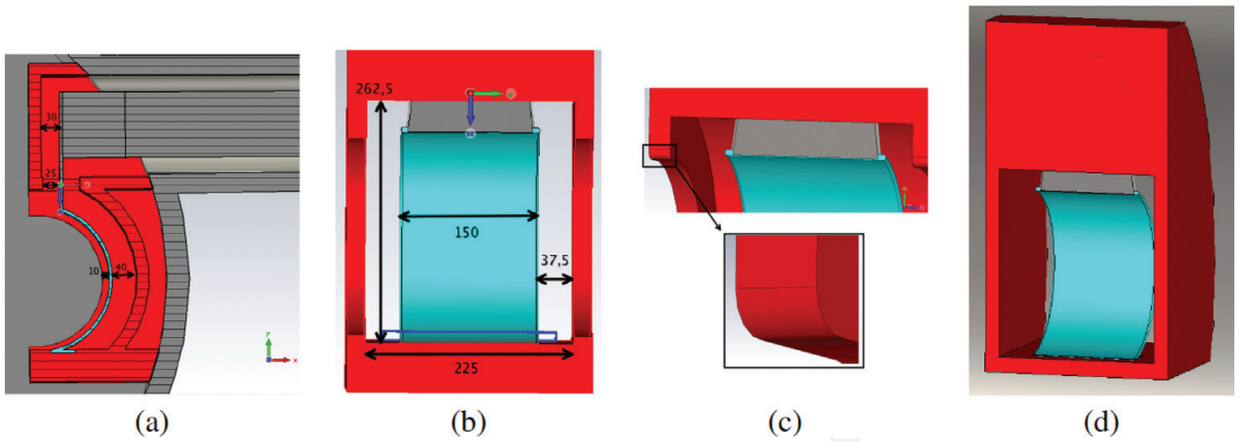

Figure 5. MicWs model of the ICRF antenna and its feeding line; (a) lateral cut view of the initial geometry; (b) front view; (c) zoom of the angular part of the limiter; (d) simplified geometry; All dimensions are given in mm.

retained geometry (with initial dimensions in mm) of the IShTAR antenna is visible in **Figure 5**. The strap is fed from the top feed through by a coaxial transmission line connected to a vertical plate inserted into the strap. Unlike usual ICRF antennas the IShTAR antenna is not designed to couple as much power as possible to the plasma, but rather to generate the typical electric fields structures expected in a tokamak. The first simulations with MWS clearly demonstrated some issues due to the presence of sharp angles in the lateral limiters. Even by further smoothing these angles (see **Figure 5c**) the electric fields maps were dominated by peaked radiations at the level of the limiters, which could also be partly due to numerical issues (meshing). We therefore decided to replace these profiled limiters by rectangular plates: see **Figure 5d**, resulting in a more regular electric field distribution. This change also considerably simplifies the building of the antenna box [16]. The antenna was installed in IShTAR and is visible in **Figure 6b**.

3.7. Diagnostics

In the present configuration, each diagnostic dedicated to physics applications has its own acquisition system. A centralised acquisition system is being built with a NI Chassis and a set of digitizer boards to offer a common time reference, shared data storage and network access. The instrumentation is still under development. At present the two main tools to diagnose plasma parameters and electric fields are probes and spectroscopy. In future other diagnostics will be added, for example an interferometer for density measurements has already been designed, in order to bench mark the data obtained by the Langmuir probes. In addition, more RF compensated probes will be added in the helical plasma source to study better the helicon physics and the effect of the magnetic topology.

The probes are depicted in **Figure 6**. Different Langmuir and B-dot probes have been installed. **Figure 6a** shows an inside view of the back flange, with an array of three probes in the middle, to the right a planar non-compensated Langmuir probe with a diameter of 2 cm can be seen. A manipulator arm (**Figure 6b**) can carry up to four probes simultaneously, which allows a partly 2D scan of the plasma profile on a shot-to-shot basis. In **Figure 6b** also the ICRF

http://dx.doi.org/10.5772/intechopen.76730

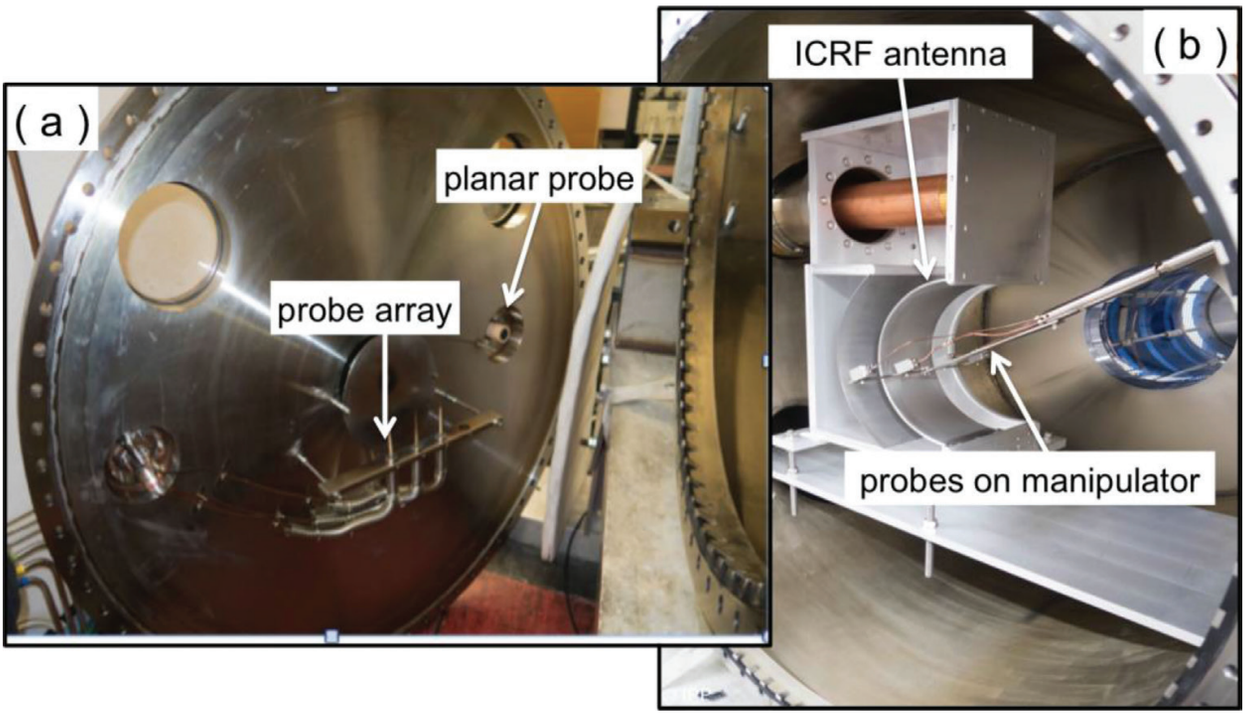

Figure 6. Inside view of the main vessel with the different probes: (a) on the back flange and (b) on a movable manipulator arm. The helical plasma source is visible on the right.

antenna can be seen, it has a single antenna strap, which is curved to follow the plasma shape. In this picture the antenna box was not yet closed and the connection to the feeding line on the top is visible. For the sheath physics, an important parameter to investigate is the electric (E) field created at the antenna and plasma facing components. The ions accelerated in the sheath potential can damage the components by creating a local overheating (hot spots) and or sputtering, as it is has been observed during ICRF experiments in different fusion machines.

After a theoretical study, two different spectroscopic methods have been retained and are presently being developed in parallel.

Passive optical spectroscopy is selected as the first approach to directly measure electric fields in the vicinity of an ICRF antenna, without disturbing the plasma environment [17–20]. This technique enables studying the perturbation of the electronic structure of an atom caused by an external electric field, the Stark effect. These perturbations are detectable as a shift of the central wavelength of a spectral line, and the occurrence of forbidden components of the fine structure in a spectral line profile. We have focused our research on the Stark effect on 4^3D - 2^3P transitions in helium. The method requires a high-resolution spectrometer with high dynamic range detector capable to resolve the allowed and forbidden lines of the transition under the study. To this end a 0.75 m Andor spectrometer equipped with an Andor ICCD camera has been installed. In the test work the He n = 4^3D - 2^3P transition has been selected for the E-field measurements, since the signal-to-noise ratio of the recorded spectra was acceptable and the line Stark broadening is strongly affected by the E-field. Once the time-averaged spectra are recorded, the spectral line profiles are compared to the simulated ones and the electric field amplitude is extracted with the method of least squares. To simulate the spectra

perturbed by an electric field, in the presence of a background magnetic field, the Explicit Zeeman Stark Spectral Simulator (EZSSS) [17] was used. This code generates the discrete spectrum by solving the Schrödinger equation in electric dipole approximation, with external electric and magnetic fields as perturbations. In the second step, by convoluting the discrete spectra with Gaussian and/or Lorentzian profiles to mimic the broadening mechanisms, the continuous spectrum is obtained.

Figure 7 depicts the modelled triplet line profile corresponding to the 4^3D - 2^3P He-I transition with no electric field externally imposed on the system. The discrete spectra, calculated with the EZSSS code is shown as a set of lines in the mirror image of the intensity scale. The continuous spectra, presented in the positive part of the intensity axes is convoluted with a Gaussian distribution corresponding to the Doppler broadening with a temperature of the radiator of 0.7 eV. The distinct feature of these spectra is the occurrence of the second spectral line red-shifted from the main component, corresponding to the fine structure of the He triplet transition. This separation of the components allows estimating the E-field in the plasma.

An alternative, but more complicated approach, is to use Doppler-free saturation spectroscopy (DFSS) to eliminate disturbing effects such as the Doppler broadening and to highlight the E-field influence [17, 21]. The basic principle is to create a cross section in the plasma of overlapping pump and probe beams from the same laser source tuned to specific absorption

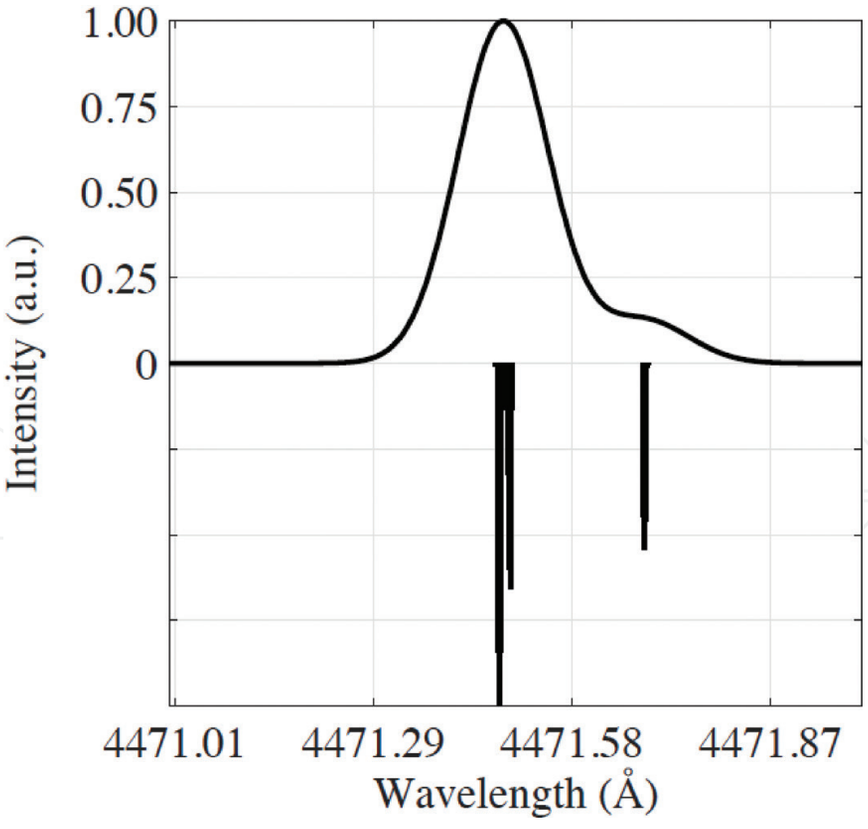

Figure 7. Triplet He-I 4^3D-2^3 P line profile simulated with the EZSSS code with no external electric field (reference scenario) shows discrete and continuous results, with the main component at wavelength λ = 4471.49 Å and the second component at 4471.6 Å.

http://dx.doi.org/10.5772/intechopen.76730

transition of He or H atoms. The pump beam depletes the ground state; the probe beam passes the plasma with reduced absorption. By depleting the ground state, the fine structure of the spectral line should become more clearly visible, in the form of local dips in the Doppler broadened absorption line. This allows measuring line profile with eliminated effect of the Doppler broadening and precisely estimate E-field with high sensitivity.

4. Operation and results as preparation for the sheath studies

4.1. Sequence of a typical discharge

A typical discharge sequence is presented in **Figure 8a**, as it is seen by the different diagnostics; one camera view is shown in **Figure 8b**. The vessel is prefilled at the operating pressure before the start of the sequence. The RF power is matched for plasma with magnetic field. Therefore the coils are usually activated before the antenna. However, the reversed sequence, as used on the discharge in **Figure 8a** shows how the magnetic field affects the plasma and the measurements of the Langmuir probe. We notice that the ion saturation current starts to ramp up only when the field is activated. On the cameras, the visible light shows that the plasma is first confined in the plasma source and then, when the coils are powered, a plasma tube develops in the main vessel and is displaced towards the centre, further away from the Langmuir probe, following the field lines represented in **Figure 3**. The minimum amount of power required to ignite the plasma was evaluated at 50 W (with and without magnetic field). During the phase without the main field, arcing is noticed in the main vessel, which is then wiped out with the start-up of the coils. No arcing has been noticed on the helicon antenna

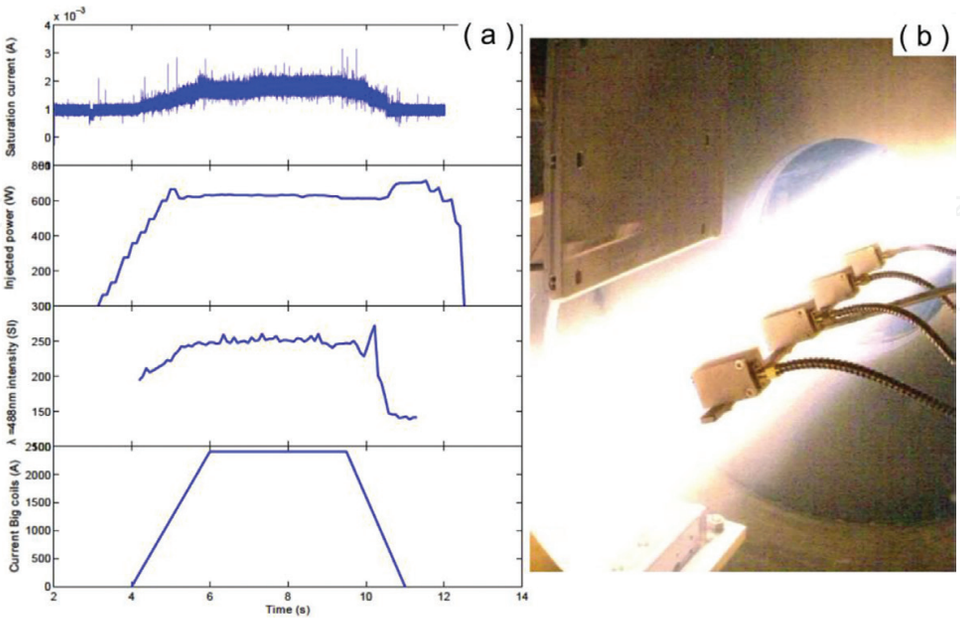

Figure 8. (a) Evolution of the main parameters for an injected helicon power of 700 W. (b) Plasma inside the main vessel in front of the ICRF antenna.

with the camera. However, post-experiment inspection revealed that the copper layer has been damaged on some parts of the line.

4.2. Characterisation and optimisation of the plasma

The operating parameters (injected RF power, neutral gas pressure and magnetic field) were scanned to observe the effect on the plasma density and temperature measured in the centre of the main vessel. The purpose is to select the set of parameters that optimises the density. The results of the parametric studies are presented in **Figure 9** [22–24]. At a constant magnetic field, the density increases almost linearly with the power. A small drop around 1.8 kW is observed, which may be due to an internal resonance. The nature of the resonance is not yet clear and needs further investigation. The optimisation of the IShTAR plasma operations is subject of on-going research. However no step in the scan is seen, which would correspond to a change of regime from inductive to helicon mode. This is probably due to a too low level of power with respect to the volume to ionise. The electron temperature does not feature any evolution inside a band between 4 and 7 eV, except for a peak at the same assumed resonance at 1.8 kW. This would confirm that the increased injected power is used to generate denser plasmas and not to heat. At constant injected power, two different trends are observed when the magnetic field is ramped up. At low pressure, the density reaches a plateau at 0.06 T and saturates before starting to drop at 0.14 T. At higher pressure, the density increases almost linearly with the magnetic field. The temperature presents a slight trend towards an increase, but there is not much difference between the high- and low-pressure cases. The cause for the saturation of the density is not yet clear and will require comparison with theoretical models, which are presently not yet available. The radial profiles of the plasma density and of the

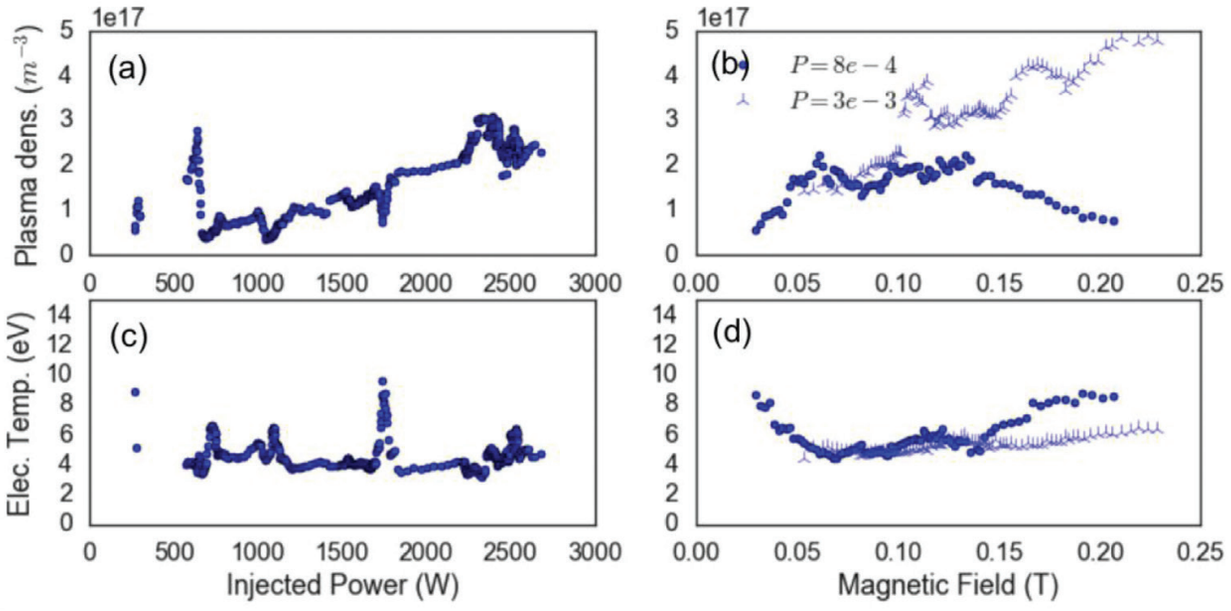

Figure 9. (a) and (c) Scan of argon plasma parameters as a function of the injected power at constant magnetic field (0.1 T) and neutral gas pressure P (10^4 mbar). (b) and (d) Plasma parameters as a function of the magnetic field at constant injected power (2.5 kW) for two levels of neutral gas pressure P (8×10^{-4} and 3×10^{-3} mbar).

http://dx.doi.org/10.5772/intechopen.76730

RF fields were measured with the manipulator over several discharges and are presented in **Figure 10** for two different magnetic fields at constant injected power of 2.5 kW and a neutral pressure of 10^{-4} mbar. The magnetic field strengths of 0.12 and 0.06 T, indicated in the figure, refer to the centre of the main vessel. The limit of 0.1 T, which was mentioned before, is for the helical plasma source. It is caused by the 1kA current limit in the small coils. The large coils around the main vessel can generate fields up to 0.4 T. The density profile has a Gaussian shape with a mean width of 10 cm, half the length of the plasma source geometrical radius. The profile does not change with the magnetic field, which corresponds to the "saturation" effect described above. Optimisation of the profile shape and peak density is still possible by adapting the magnetic field strength and topology. It seems to be connected to the helicon wave dispersion relation. A detailed study is on-going in order to create the best possible conditions at the location of the ICRF antenna to be relevant for the intended sheath studies.

In the last set of experiments high-resolution passive optical emission spectroscopy was used to estimate an E-field in typical conditions of the IShTAR device operation [18]. To detect the expected Stark-effect-induced changes on the spectral line profile two experimental scenarios have been performed to obtain the results presented here. The reference data were recorded without the voltage applied to the electrode placed directly in the Helicon source, while the second set was obtained for the set of experiments with the electrode biased to a positive DC-voltage of U_{el} = 1 kV. The obtained line profiles corresponding to the 4^3D - 2^3P transition in He-I were recorded over the whole duration of a discharge, with an exposure time of 0.5 s, in a kinetic series of 24 scans per discharge. The processed data shows a reproducible shift of the He-I 4^3D - 2^3P line (**Figure 11**) when the external electric field is present in the thermal sheath in front of the DC-biased electrode. For a rough estimate of the electric field expected in a thermal sheath in front of the electrode we can assume that it originates from the difference in potentials between the electrode and the plasma, over the distance corresponding to the sheath thickness. Compared to the potential applied on the electrode, U_{el} = 1 kV, the plasma potential is U_{pl} = 0 kV. The sheath thickness corresponding to the density of helium plasma in IShTAR of $n_e = 10^{16}$ m^{-3}, and the electron temperature of T_e = 5 eV is proportional to the Debye length of $\lambda_D = 5\times10^4$ m. Therefore the electric field in the vicinity of the electrode biased to U_{el} = 1 kV, can be estimated to be the applied voltage drop over the sheath thickness. To complete the

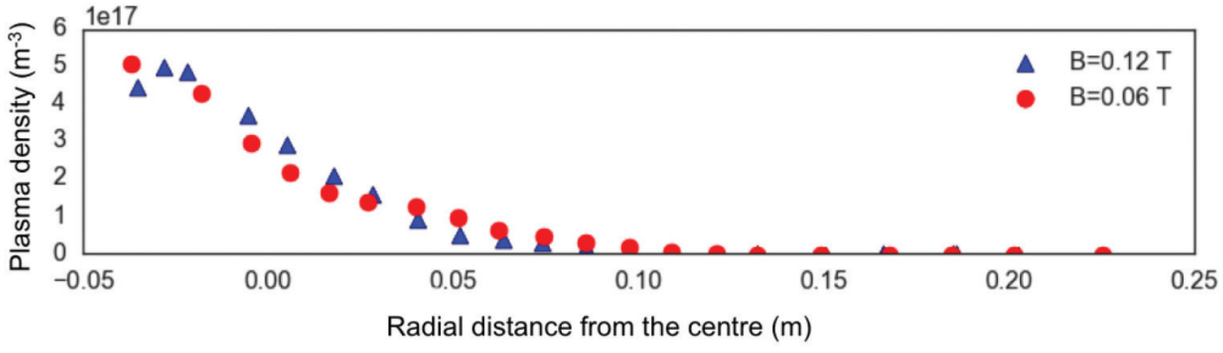

Figure 10. Radial profile measurements of the plasma density. The magnetic field strengths refer to centre of the main vessel.

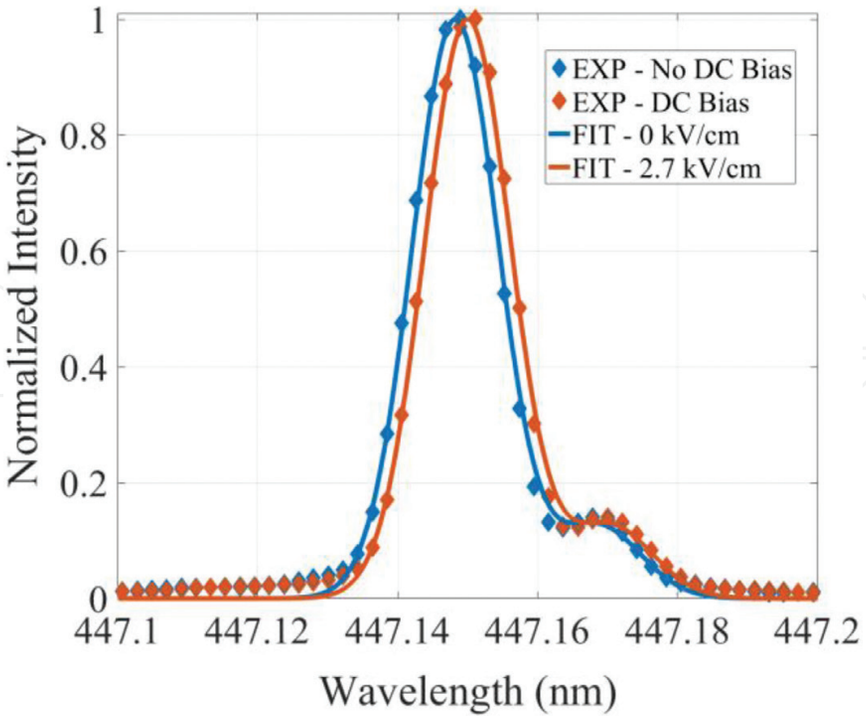

Figure 11. Experimental 4^3D-2^3 P He I line profile for E_{DC} = 0 kV/cm and E_{DC} = 2.7 kV/cm (black and red diamonds, respectively) fitted with the simulated theoretical spectra calculated with the EZSSS code (solid lines).

study, the He-I 4^3D - 2^3P transition is simulated with the EZSSS code for several values of the DC electric field, and the best match between the measured and simulated lines corresponds to a simulated spectral line exposed to the external electrical field of E = 2.7 kV/cm, as depicted in **Figure 3** with the solid lines. The estimated electrical field agrees with theoretical prediction and showing possibility of passive emission spectroscopy with high resolution to be used for E-field measurements [16, 17].

5. Conclusions and future plans

A dedicated test facility has been constructed for studying RF sheath effects [24]. For this purpose plasma conditions representative of the edge of a tokamak are needed. A helical antenna creates plasmas with the required parameters. Helium and argon operation are used routinely, also hydrogen is foreseen, as well as gas mixtures. Plasma densities of the order of 10^{17}–10^{18} m^{-3} and temperatures around 5–10 eV have been obtained. The main limiting factor is the generator power (3 kW) of the helical antenna. Performance optimisation is possible by adapting the magnetic field strength and topology; the detailed study of the helical plasma source will be the subject of future research.

A simple ICRF antenna is installed and operational, it is coupled to a broadband generator with frequencies in the range of 100 kHz to 100 MHz and a maximal power of 1 kW. If needed

in the future a much more powerful generator can be used, when it will be coupled to the ASDEX RF system, with an available power up to the MW level.

Attention is also given to developing diagnostics for characterising the plasma parameters and electric fields, especially in the vicinity of the ICRF antenna, since they are the key ingredients for the sheath theories and modelling codes. Different probes and spectroscopic methods are used.

With the probes the behaviour of the plasma electron density and the three magnetic field components of the injected RF fields are measured under different operating conditions. Modelling is on-going using the COMSOL multi-physics environment [25, 26]. The measurements will also serve more advanced sheath and edge simulation codes in the future.

For measuring electric fields in the plasma caused by the RF antenna sheaths two approaches are followed. Passive optical emission spectroscopy monitors Stark effects on spectral lines with a high-resolution spectrometer, provided that the local electric fields are strong enough to overcome the broadening of the lines. Doppler-free saturation spectroscopy is more powerful; a laser beam depletes the ground state, eliminates the line broadening effects and makes smaller electric fields visible. However, the more complicated set-up, with a careful alignment of laser beams, makes the measurements much more challenging. After a first test on a glow discharge plasma, the design of the optical path and the installation of the laser at IShTAR have started.

Acknowledgements

The authors want to thank the technical staff at IPP - Garching, LPP-ERM/KMS and Ghent University, in particular F. Fischer, G. Siegl, M. Berte and J. Peelman.

Conflict of interest

There are no conflicts of interest.

Notes/Thanks/Other declarations

The work received support from the Research Foundation Flanders (G0B3115N). This work has been carried out within the framework of the EUROfusion Consortium and has received funding from the Euratom research and training programme 2014–2018 under grant agreement No 633053. The views and opinions expressed herein do not necessarily reflect those of the European Commission.

Author details

Kristel Crombe[1,2]*, Rodolphe D' Inca[3], Eric Faudot[4], Helmut Faugel[3], Ana Kostic[3], Mariia Usoltceva[4], Jean-Marie Noterdaeme[3], Anton Nikiforov[1,3], Helmut Fuenfgelder[2], Stephane Heuraux[1], Jonathan Jacquot[3], Fabrice Louche[3], Roman Ochoukov[1,3,4], Ilya Shesterikov[2] and Dirk Van Eester[1,3]

*Address all correspondence to: kristel.crombe@ugent.be

1 Department of Applied Physics, Ghent University, Ghent, Belgium

2 Laboratory for Plasma Physics, ERM-KMS, Brussels, Belgium

3 Max-Planck-Institut fuer Plasmaphysik, Garching, Germany

4 Université de Lorraine, France

References

[1] Chen FF. High Density Plasma Sources. 1st ed. USA: William Andrew; 1995

[2] Noterdaeme J.-M, Van Oost G. The interaction between waves in the ion cyclotron range of frequencies and the plasma boundary. Plasma Physics and Controlled Fusion. 1993;**35**:1481 and references therein

[3] Bobkov V et al. ICRF operation with improved antennas in ASDEX upgrade with W wall. Nuclear Fusion. 2013;**53**(9):093018

[4] Jacquet P et al. Ion cyclotron resonance frequency heating in JET during initial operations with the ITER-like wall. Physics of Plasmas. 2014;**21**:061510

[5] Klepper CC et al. RF sheath-enhanced beryllium sources at JET's ICRH antennas. Journal of Nuclear Materials. 2013;**7**(438):S594-S598

[6] Lerche E et al. Impact of minority concentration on fundamental (H)D ICRF heating performance in JET-ILW. Nuclear Fusion. 2014;**54**(7):073006

[7] Colas L et al. Self-consistent radio-frequency wave propagation and peripheral direct current plasma biasing: Simplified three-dimensional non-linear treatment in the "wide sheath" asymptotic regime. Physics of Plasmas. 2012;**19**:092505

[8] Crombé K et al. Studies of RF sheaths and diagnostics on IShTAR. AIP Conference. Proc. 1689, Proceedings of the 21st Topical Conference on Radiofrequecy Power in Plasmas, UCLA Conference Center at Lake Arrowhead, California 2015. 030006

[9] Crombé K et al. Coupled and decoupled solutions of the cold plasma dispersion relation. Journal of Plasma Physics. 2016;**82**:905820203

[10] Tripsky M et al. Discharge initiation by ICRF antenna in IShTAR. EPJ Web of Conferences. 2017;**157**:03056

[11] Raizer YP, Kisin VI, Allen JE. Gas Discharge Physics. Vol. 1. Berlin: Springer-Verlag; 1991

[12] Lieberman MA, Lichtenberg AJ. Principles of plasma discharges and materials processing. MRS Bulletin. 1994;**30**:899

[13] Miao TT et al. The study of helicon plasma source. Review of Scientific Instruments. 2010;**81**(2):02B105

[14] Chen FF, Boswell RW. Plasma Science. IEEE Transactions. 1997;**25**:1245

[15] CST STUDIO SUITE®, CST AG, Germany, www.cst.com

[16] Louche F et al. Designing the IShTAR antenna: Physics and engineering aspects. AIP Conference Proc. 1689. In: Proceedings of the 21st Topical Conference on Radiofrequency Power in Plasmas. UCLA Conference Center at Lake Arrowhead, California. 2015

[17] Martin EH. Electric Field Measurements of the Capacitively Coupled Magnetized RF Sheath Utilizing Passive Optical Emission Spectroscopy [PhD thesis]. North Carolina State University; 2014

[18] Kostic A et al. Feasibility study of passive optical emission spectroscopy for the electric field measurements in IShTAR. EPJ Web of Conferences. 2017;**157**:03025

[19] Crombé K et al. Helium operation of IShTAR in preparation of E-field measurements. ECA. 2017;**41F**:5-144

[20] Lee C, Graves D, Lieberman M, Hess D. Journal of the Electrochemical Society. 1994;**141**:1546

[21] Wieman C, Hansch T. Doppler-free polarization spectroscopy. Physical Review Letters. 1976;**17**:1170

[22] D'Inca R, Jacquot J, et al. Development and first operations of the IShTAR test facility. In: 42nd EPS Conference on Plasma Physics (EPS), Vol. 39E; Lisbon, Portugal: ECA. 2015. P1.154

[23] D'Inca R, Kostic A, et al. Characterization of the RF plasma on the IShTAR testbed. In: 43rd EPS Conference on Plasma Physics, Vol. 40A; 4-8 July 2016; Leuven, Belgium: ECA. 2016. O5.129

[24] Crombé K et al. Characterization of the RF plasma on the IShTAR testbed. In: 22nd IAEA FEC Conference; 17-22 October 2016; Kyoto, Japan

[25] Usoltceva M et al. IShTAR: A helicon plasma source to characterize the interactions between ICRF and plasma. In: COMSOL Conference; 12-14 October 2016; München, Germany

[26] Usoltceva M et al. IShTAR ICRF antenna field characterization in vacuum and plasma by using probe diagnostic. EPJ Web of Conferences. 2017;**157**:03058

IntechOpen